Heterodyne AC Kelvin Probe Force Microscopy for Nanoscale Surface Potential Imaging in Liquids

Thomas Hackl, Mathias Poik, and Georg Schitter Senior Member, IEEE

***Abstract*—Knowledge of electric charge and potential distributions at the nanoscale is of great interest in the fields of material science and biology. The required high measurement accuracy, spatial resolution and applicability to aqueous environments is not always provided by conventional techniques such as Kelvin Probe Force Microscopy due to averaging artefacts and the use of a dc bias. This paper presents the development of an Atomic Force Microscopy measurement mode, enabling quantitative surface potential measurements of nanoscale structures with high measurement accuracy in air and liquid (aqueous) environments. Averaging artefacts caused by the influence of cantilever cone, cantilever beam and tip-sample distance in dc-bias-free Kelvin Probe Force Microscopy (AC-KPFM) are eliminated by the implemented heterodyne detection and single-pass operation. The accuracy of the potential measurement as compared to amplitude modulated KPFM modes is greatly improved, while keeping the advantages of closed-loop and dc-bias-free operation. Experiments on a gold-aluminum test-sample and collagen fibrils show quantitative surface potential measurements on nanoscale structures and operability in aqueous environment.**

***Index Terms*—kelvin probe force microscopy, surface potential, heterodyne detection, aqueous environment**

I. Introduction

KELVIN probe force microscopy (KPFM) [1] is an atomic force microscope (AFM) measurement mode for the determination of the local electric surface potential distribution. Electric potentials and charge distributions at the nanoscale are important surface properties as they strongly affect the physical and chemical interaction of the carrier with its environment. KPFM has therefore been used in a variety of scientific fields, such as corrosion studies [2], [3], analysis of semiconductors [4], [5], study of photoconducting devices [6] or biological applications [7], [8]. Common to these applications is that they require a high spatial resolution due to the inherently nanoscale structures (e.g. semiconductor structures, biomolecules). Additionally, measurements in aqueous environments gained importance in the recent years [9], as it represents the natural surrounding of corrosion processes or biological substances. Here, possible electrochemically induced effects pose challenges to these electrical AFM measurements. Possible damage to the sample and its environment must be avoided with the application of suitable electrical signals.

Many variants of KPFM have evolved [9] most of which use a dual-pass technique (interleaved scan), where the topography of each scan line is recorded in a first step. The surface potential distribution is then mapped in a subsequent step, where the sample topography is retraced at a constant tip-sample distance (i.e. lift height). The surface potential is measured by modulating the electrostatic interaction of the conducting cantilever to the sample by the application of an ac voltage. The electrostatic force acting on the tip is nullified by adjusting an additional dc voltage U_{DC} between the cantilever and the sample, directly leading to the surface potential $\phi = U_{DC}$. This amplitude modulated KPFM (AM-KPFM) is sensitive to the long-range electrostatic force acting on the cantilever. The measurement is therefore not only influenced by the local surface potential at the tip apex, it also includes unwanted contributions of sample structures beneath the cantilever cone and beam, decreasing its spatial resolution [10]. Additionally, the lift height choice determines the contribution of each cantilever part on the overall electrostatic force, resulting in an unreliable surface potential measurement. This issue is generally known as averaging effect in AM-KPFM modes. More importantly, the use of a dc bias during the measurement prevents its use in aqueous environments. The dc electric field between sample and cantilever can never be fully compensated, due to non-uniform charge distribution on the sample, leading to electrochemical reactions or gas formation (i.e. electrolysis [11]) with the associated irreversible damage to the sample and its surroundings.

Other variants of KPFM, with frequency modulated- (FM) [12] and heterodyne- (H) [13] detection techniques, have been developed. These modes are sensitive to the gradient of the electrostatic force acting on the cantilever, which has a shorter range than the electrostatic force itself [14]. Therefore, the contribution of the cantilever beam and cone is mitigated, which in turn increases the spatial resolution. Additionally, their implementation of different drive and detection frequencies prevents possible capacitive signal crosstalk within the AFM [15] from interfering with the measurement, which is an issue in AM-KPFM [16]. Another approach to mitigate averaging artefacts and poor spatial resolution in KPFM is to omit the use of the dual-pass scan and to measure the topography and surface potential in a single-pass configuration simultaneously [17]. The advantage lies in the reduced tip-sample distance during the potential measurement, contributing to increased spatial resolution. Usual implementations use the resonance frequency of the cantilever for the surface potential measurement, while the topography scan operates at its first overtone in order to impede any interference or crosstalk between the measurement signals. While these mentioned methods enable accurate surface potential measurements at the nanoscale, they still use a dc voltage for the nullification of the electrostatic

The financial support by the Austrian Science Fund FWF (Project Nr. P 31238-N28) and the Austrian Research Promotion Agency FFG (Project Nr. 883916) is gratefully acknowledged. *(Corresponding author: Thomas Hackl.)*
The authors are with the Automation and Control Institute (ACIN), Technische Universität Wien, 1040 Vienna, Austria (e-mail: hackl@acin.tuwien.ac.at).

Post-Print version of the article: T. Hackl, M. Poik and G. Schitter, "Heterodyne AC Kelvin Probe Force Microscopy for Nanoscale Surface Potential Imaging in Liquids," *IEEE Transaction on Instrumentation and Measurement*, 2023. DOI: 10.1109/TIM.2022.3230477

force, making them unsuitable for operation in liquid or more specific aqueous environments.

There have been efforts to bypass the need for a dc-bias by using open-loop methods [18], [19]. However, such open-loop techniques require an accurate calibration before each measurement. Possible tip pick-up (an issue when imaging biological samples [20]) or temperature drifts can make this calibration invalid, leading to hard to interpret or flawed measurements. Recently the possibility of dc-bias-free closed-loop KPFM has been demonstrated. It uses a second, modulated ac voltage instead of the dc-bias for the nullification of the electrostatic force and is known as AC-KPFM [21]. Stable closed-loop operation of AC-KPFM in aqueous environment has been shown without the induction of any parasitic electrochemical effect [22]. However, since AC-KPFM is again sensitive to the electrostatic force it can be categorized to amplitude modulated (AM) techniques with all its aforementioned drawbacks.

The contribution of this article is the development of a novel AFM method, enabling quantitative measurements of electric surface potentials in air and liquid environments with nanoscale resolution. This article is an extension of our previous work [23], which combined AC-KPFM with a heterodyne detection. It used conventional dual-pass operation, featuring limited spatial resolution and accuracy and focused on the evaluation on test structures in air with no verification in liquids. The method presented here operates in single-pass, which improves spatial resolution and measurement speed as the tip-sample distance is minimized and the sample topography and surface potential are measured simultaneously. The developed mode is demonstrated and compared against conventional techniques on several nanoscale test structures to assess its quantitative measurement capability. Further, measurements on actual biological samples (collagen fibrils) are carried out, demonstrating nanoscale resolution and applicability to aqueous environments.

II. Principle of Heterodyne AC-Kpfm for Liquids

In this section, the AC-KPFM [21] technique is presented first, which is then extended by the heterodyne detection and single-pass operation. Fig. 1(a) shows the setup of AC-KPFM (switch position: down) as well as heterodyne AC-KPFM (switch position: up), which is referred to as HAC-K-L *(Heterodyne AC-Kpfm in Liquids)* in the following. In their original form, these methods operate in a dual-pass mode (see Fig. 2), where in the first pass the topography of a scan line is measured with conventional techniques, such as contact or intermittent contact mode. Subsequently the cantilever follows the recorded topography at a constant distance to the sample and the surface potential is measured. In AM-KPFM an ac voltage (amplitude: a; frequency: ω_{el}) with a dc offset: $U_C = U_{DC} + a \cdot sin(\omega_{el}t)$ is applied to the conducting cantilever in the second pass, whereas AC-KPFM replaces this dc-bias with an additional sinusoidal signal of twice the frequency (amplitude: b):

$$U_C = a \cdot sin(\omega_{el}t) + b \cdot cos(2\omega_{el}t). \tag{1}$$

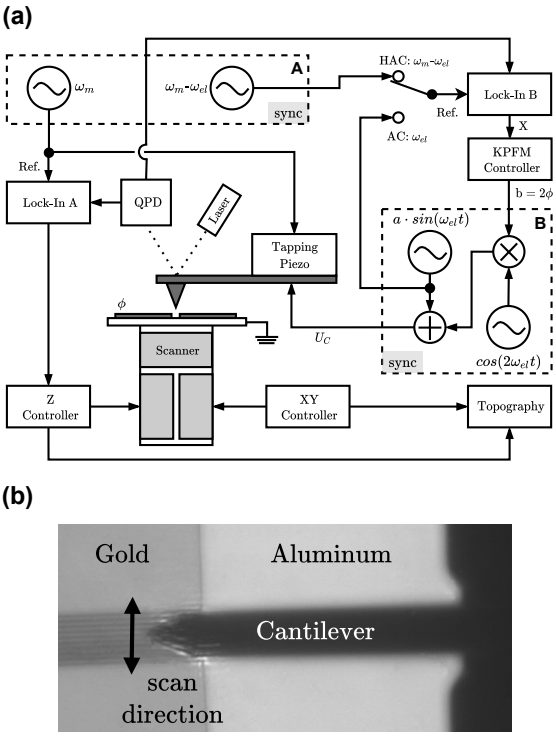

Fig. 1. (a) Implemented HAC-K-L setup with the added components on the top and right side. Signal generator A is used for the topography scan, to mechanically excite the cantilever and to provide the reference frequencies (ω_m, ω_m-ω_{el}) to the lock-in amplifiers. A KPFM controller modulates amplitude b of signal generator B, which provides U_C. The signal b is recorded and used in a post-processing step to calculate the surface potential map $\phi = b/2$. (b) Camera view of the setup with the cantilever and the gold-aluminum test sample underneath as used in the experiments.

The electrostatic force F_{el} acting on the tip-sample system is usually expressed as a capacitor model:

$$F_{el} = \frac{1}{2}\frac{\partial C}{\partial z}(\phi - U_C)^2, \tag{2}$$

where $\partial C/\partial z$ is the capacitance gradient between the tip and the sample at the separation z, ϕ is the local surface potential to be measured and U_C the applied voltage on the cantilever. Inserting (1) into (2) leads to various electrostatic force components at several frequencies:

$$F_{el} = \frac{1}{2}\frac{\partial C}{\partial z}\left\{\begin{array}{ll} \phi^2 + \frac{a^2+b^2}{2} & \\ +a\left[2\phi - b\right] & sin(\omega_{el}t) \\ -\left[2\phi b + \frac{a^2}{2}\right] & cos(2\omega_{el}t) \\ +ab & sin(3\omega_{el}t) \\ +\frac{b^2}{2} & cos(4\omega_{el}t) \end{array}\right\}. \tag{3}$$

AC-KPFM determines the surface potential ϕ by measuring the cantilever deflection amplitude at the frequency ω_{el} (Lock-In B in Fig. 1(a)). A feedback controller is then used to nullify $F_{\omega_{el}}$ by adjusting amplitude b, such that $b = 2\phi$. The recorded signal b is then used in a post-processing step to calculate the surface potential $\phi = b/2$. To make use of

Post-Print version of the article: T. Hackl, M. Poik and G. Schitter, "Heterodyne AC Kelvin Probe Force Microscopy for Nanoscale Surface Potential Imaging in Liquids," *IEEE Transaction on Instrumentation and Measurement*, 2023. DOI: 10.1109/TIM.2022.3230477

the high Q-factor of AFM cantilevers and to thus increase the signal-to-noise ratio (SNR), ω_{el} is usually set to the resonance frequency of the cantilever. Next to the advantage that AC-KPFM is dc-bias-free, it also features twice the control sensitivity as compared to conventional AM-KPFM. However, AC-KPFM is equally sensitive to the electrostatic force (see (3)) and features therefore a poor spatial resolution, a lift height dependence and limited surface potential accuracy arising from the averaging effect.

Heterodyne detection is achieved by exciting the cantilever not only electrically by the application of U_C, but also mechanically during the surface potential measurement. By driving the dither piezo at the frequency ω_m the separation z of the cantilever to the sample can be modelled as:

$$z = \bar{z} + A \cdot sin(\omega_m t), \tag{4}$$

where A is the amplitude of the cantilever deflection at ω_m and $\bar{z}$ is the mean lift height of the cantilever in the interleave scan. The Taylor-Expansion of the tip-sample capacitance gradient is therefore [24]:

$$\frac{\partial C}{\partial z} \approx \frac{\partial C}{\partial z}\bigg|_{\bar{z}} + A \cdot \frac{\partial^2 C}{\partial z^2}\bigg|_{\bar{z}} \cdot sin(\omega_m t). \tag{5}$$

Inserting the altered capacitance gradient (5) into (3) results in frequency mixing of the mechanical and electrical excitation at ω_m and ω_{el}, respectively. The force term at ω_m-ω_{el} is used in this implementation and has the following form:

$$F_{\omega_m\text{-}\omega_{el}} = \frac{A}{4}\frac{\partial^2 C}{\partial z^2}\bigg|_{\bar{z}} \cdot a(2\phi - b) \cdot cos[(\omega_m\text{-}\omega_{el})t]. \tag{6}$$

This electrostatic force term leads to a deflection of the cantilever, which again is nullified by controlling b, such that $b = 2\phi$. In contrast to AC-KPFM, the measurement is sensitive to the second derivative of the tip-sample capacitance, which is equivalent to the electrostatic force gradient, instead of the electrostatic force itself. Therefore, heterodyne AC-KPFM mitigates the contribution of the cantilever cone and beam and thus improves the spatial resolution. From (6) follows that a large mechanical drive amplitude A is favourable in order to get a good SNR. This can be achieved by setting ω_m to the second flexural mode of the cantilever, while keeping ω_m-ω_{el} at the fundamental resonance frequency, by an appropriate choice of ω_{el}. However, the sole implementation of heterodyne detection is still not accurate enough to quantitatively image nanoscale structures, which becomes more evident in the experimental section. A further increase in spatial resolution of the measurement can be achieved by reducing the tip-sample distance during the potential measurement as can be seen in Figure 2. Since the heterodyne detection requires a mechanical cantilever excitation, directly making use of the oscillation during the topography scan proves to be useful. This not only enhances the SNR and spatial resolution, since the mean tip-sample distance $\bar{z}$ is at its minimum (Fig. 2) and therefore $\partial^2 C/\partial z^2$ at its maximum, it also doubles the measurement speed as the interleave scan is no longer required. An eventual crosstalk between the topography- and the surface potential measurement can be neglected as the two modes operate

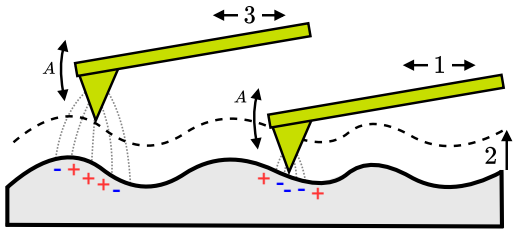

Fig. 2. Principle of dual-pass (1-2-3) and single-pass (1) operation. In single-pass operation, the mechanical cantilever oscillation with the amplitude A of the topography measurement (intermittent contact mode) is directly used for heterodyne detection in HAC-K-L.

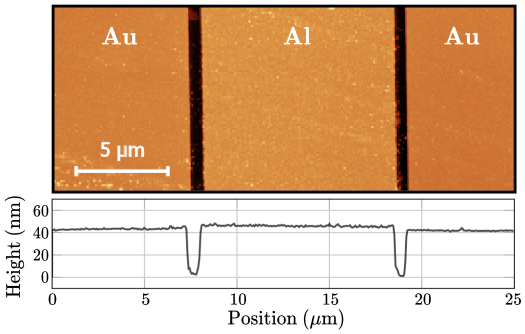

Fig. 3. Topography image of the used sample with stripes of varying metals (gold-aluminum). A representative height profile is shown for clarity.

on different frequencies (ω_m, ω_m-ω_{el}) usually separated by tens of kHz. Additionally, the nullifying principle of the closed-loop operation ensures negligible cantilever oscillation caused by the electrostatic force ($F_{\omega_m\text{-}\omega_{el}} \cong 0$). In terms of setup complexity, the introduced technique is comparable to conventional KPFM modes. It can be upgraded to existing AFM systems using standard hardware components like lock-in amplifiers, signal generators and controllers.

III. Setup and Experimental Details

The setup in Fig. 1 is implemented on a commercial AFM (Multimode 8, Bruker, USA) using external signal generators (33522B, Keysight Technologies, USA) for providing U_C, to mechanically excite the cantilever and to provide the reference frequencies to the lock-in amplifiers. The external lock-in-amplifier Lock-In B (SR844, Stanford Research Systems, USA) is used to demodulate the cantilever deflection. Its bandwidth is set to 10 kHz and kept constant throughout all measurements. A proportional-integral (PI) controller (KPFM controller) implemented on a rapid prototyping system (DS1005, dSpace, Germany) is used to modulate the amplitude b of U_C, in order to nullify the demodulated in-phase deflection amplitude (X). The AFM further consists of a Nanoscope V controller and a signal access module (SAM) for the access of specific signals, e.g. the cantilever deflection. The amplitude b is recorded and used alongside the topography scan in a post-processing step to generate the surface potential map: $\phi = b/2$. Overall gold coated cantilevers (4XC-GG, Mikromasch, USA)

Post-Print version of the article: T. Hackl, M. Poik and G. Schitter, "Heterodyne AC Kelvin Probe Force Microscopy for Nanoscale Surface Potential Imaging in Liquids," *IEEE Transaction on Instrumentation and Measurement*, 2023. DOI: 10.1109/TIM.2022.3230477

with a nominal tip radius of 30 nm, a resonance frequency of f_0 = 79.8 kHz and a nominal stiffness of k = 2.5 N/m are used in all measurements. For the topography measurement, which is done in intermittent contact mode, and the mechanical excitation in the interleave scan, a driving frequency of $\omega_m = 2\pi\cdot$ 494 kHz is selected, as the second flexural eigenmode of the cantilever is determined at this frequency. For heterodyne operation (HAC-K-L), the electrical excitation is applied at $\omega_{el} = 2\pi\cdot$ 414.2 kHz with an amplitude a = 2 V, resulting in a force component at ω_m-$\omega_{el} = 2\pi\cdot$ 79.8 kHz, the resonance frequency of the cantilever. For the use of AC-KPFM an electrical drive frequency of $\omega_{el} = 2\pi\cdot$ 79.8 kHz with the same amplitude a = 2 V is used. However, the choice of which mode operates on which cantilever-eigenmode is not predefined and can be chosen freely. This only affects the SNR and has no impact on the general working principle [25].

The method is first verified on a test-sample (KPFM & EFM Sample, BudgetSensors, Bulgaria), which features stripes of alternating materials (aluminum and gold) on an oxide covered silicon substrate separated by a ∼500 nm wide trench. The height of the stripes is almost identical (see Fig. 3), therefore minimizing possible topographical crosstalk caused by the sample. A surface potential contrast arises from the different work functions of the materials, creating a contact potential difference (CPD). Additionally an external bias can be applied to either material to set a known potential difference. Furthermore measurements on a nanoscale biological sample in air and aqueous solution are carried out. To this end, collagen fibrils are prepared from rodent tail tendon [26] and deposited on a bare n-doped silicon substrate. After measurements at ambient conditions in air, the sample and cantilever are immersed in highly deionized water (milli-Q water, Millipore, USA) using a liquid-cell (MTFML, Bruker, USA) together with an o-ring for sealage. Due to increased damping and effective mass in water, the resonance frequencies of the cantilever changes. The driving frequencies are therefore adjusted to $\omega_m = 2\pi\cdot$ 267 kHz and $\omega_{el} = 2\pi\cdot$ 219 kHz.

IV. Experimental Results

A. Lift height dependence in Dual-pass operation

Fig. 4(a) shows the measured surface potential in dual-pass operation, when sweeping the lift height from 25 nm up to 300 nm for conventional AC-KPFM (i) and HAC-K-L (ii). The cross sections (b) reveal a clear dependence on lift height when operating with AC-KPFM. As discussed in the introduction, the long-range electrostatic force not only acts on the tip apex but also on the cantilever cone and beam. In the experiment the cantilever beam extends mainly over the Al-pad (Fig. 1(b)). Meaning, that when increasing the distance to the surface and therefore also the contribution of the beam, the measured potential on the Au-pad approaches the value of the Al-pad. A careful choice of the lift height and the cantilever direction is therefore essential, when operating with amplitude modulated KPFM modes to deal with this cantilever and lift height induced artefact. With the heterodyne detection on the other hand this dependence on the lift height is greatly reduced due to its proportionality to the more localized electrostatic force gradient. Even at large distances (i.e. 300 nm) above the sample it provides the same quantitative result as for small lift heights and is thus less prone to variations of measurement parameters. Along with this advantage comes a drawback of the heterodyne detection. As the electrostatic force gradient features a rapid decline away from the surface, large lift heights lead to small forces and therefore a reduced SNR. However, the SNR can be noticeably enhanced by either increasing the mechanical or the electrical drive amplitude A and a,

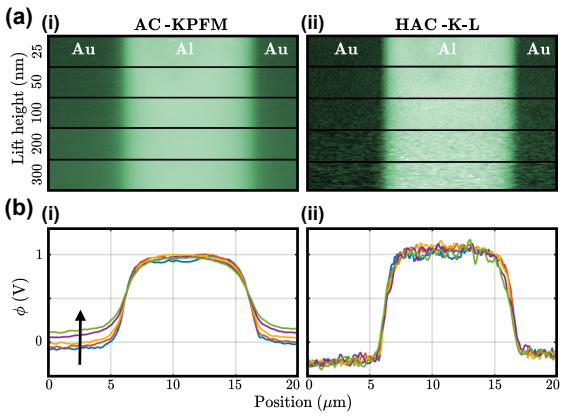

Fig. 4. (a) Sweep of the lift height (i.e. tip-sample distance) during the surface potential measurement on the Au-Al-Au sample in air using (i) AC-KPFM and (ii) HAC-K-L. (b) Cross sections for each segment in the recorded images, where the arrow denotes the direction of increasing lift height. The choice of the tip-sample distance in dual-pass operation has a major impact on the measurement result of force-sensitive AC-KPFM, whereas with the heterodyne detection this artefact is not present.

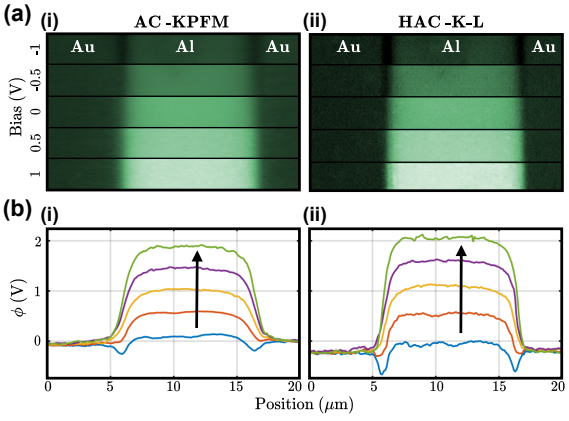

Fig. 5. (a) Sweep of the externally applied bias voltage on the Al pad, while keeping the Au potential on ground in air for (i) AC-KPFM and (ii) HAC-K-L (lift height = 25 nm). (b) Cross sections for each segment in the recorded images, where the arrows denote the direction of increased bias. Due to averaging in amplitude modulated AC-KPFM the applied voltages are not accurately measured as the difference of the -1 V and +1 V lines on the Al pad is less than 2 V, which is greatly improved with the heterodyne detection.

Post-Print version of the article: T. Hackl, M. Poik and G. Schitter, "Heterodyne AC Kelvin Probe Force Microscopy for Nanoscale Surface Potential Imaging in Liquids," *IEEE Transaction on Instrumentation and Measurement*, 2023. DOI: 10.1109/TIM.2022.3230477

respectively (as described by (6)) or by minimizing the lift-height through single-pass operation as discussed in section C.

B. Voltage accuracy and spatial resolution

Fig. 5 shows the measured surface potential on the same position as in the previous section at a lift height of 25 nm when sweeping the external bias voltage on the Al-pad, while keeping the Au-pad at ground potential. With AC-KPFM the measured surface potential between the +1 V and -1 V plateau on the Al-pad is clearly less than 2 V. This is again attributed to the averaging effect present in amplitude modulated KPFM modes. Additionally, capacitive signal crosstalk [27] can induce an offset in the feedback loop, leading to erroneous results. With HAC-K-L on the other side the detection frequency (ω_m-ω_{el}) differs from the drive frequencies (ω_m, ω_{el}). Eventual crosstalk is therefore not interfering with the measurement, as it is filtered by the narrow bandwidth of the lock-in-amplifier leading to more accurate potential values. In addition, the heterodyne detection indicates an increased spatial resolution visible through the more pronounced dip in the -1 V potential curve. It arises from the different work function of the underlying oxide covered silicon substrate that is exposed at the transition. The increased resolution can also be seen by the steeper transition of the other curves. The rise width (10 % - 90 %) of the measured surface potential (+1 V) is determined to be 1.99 µm for AC-KPFM and 1.25 µm for HAC-K-L, which is an improvement of 37% at a lift height of 25 nm.
However, in order to quantitatively image nanoscale structures an even higher level of detail and accuracy is required, as discussed in the next section with the implementation of single-pass operation.

TABLE I
DEVIATION OF THE MEASURED SURFACE POTENTIAL DIFFERENCE (AU-AL) TO THE APPLIED BIAS AND RMS NOISE OF THE INDIVIDUAL MODES (EXTRACTED FROM FIG 6(C)).

AC-KPFM Dual-pass

Bias (V)	CPD (mV)	σ (mV)
1.00	-316	3.1
0.75	-162	2.7
0.50	-5	2.9
0.25	150	2.9
0.00	304	2.9
-0.25	458	3.4
-0.50	612	3.3
-0.75	764	3.2
-1.00	916	2.9
	span: 1232	**$\bar{\sigma}$: 3.0**

AC-KPFM Single-pass

Bias (V)	CPD (mV)	σ (mV)
1.00	13	4.3
0.75	127	3.0
0.50	240	3.0
0.25	355	3.1
0.00	465	3.1
-0.25	582	3.5
-0.50	701	3.2
-0.75	819	3.1
-1.00	939	3.4
	span: 926	**$\bar{\sigma}$: 3.3**

HAC-K-L Dual-pass

Bias (V)	CPD (mV)	σ (mV)
1.00	326	29.1
0.75	356	28.2
0.50	387	28.9
0.25	400	28.6
0.00	423	27.8
-0.25	476	27.9
-0.50	492	27.7
-0.75	518	27.8
-1.00	551	29.1
	span: 225	**$\bar{\sigma}$: 28.3**

HAC-K-L Single-pass

Bias (V)	CPD (mV)	σ (mV)
1.00	498	16.4
0.75	487	17.8
0.50	493	16.4
0.25	484	16.3
0.00	500	18.4
-0.25	501	15.9
-0.50	508	16.1
-0.75	506	15.4
-1.00	522	15.8
	span: 38	**$\bar{\sigma}$: 16.5**

C. Dual-pass vs. Single-pass

Figure 6(a) shows the comparison of AC-KPFM (i,ii) and HAC-K-L (iii, iv) for both, dual- and single-pass configuration. In order to check the capability of either mode to correctly quantify the surface potential at nanoscale structures, the narrowest Au-Al-Au test structure of the sample is used (Al

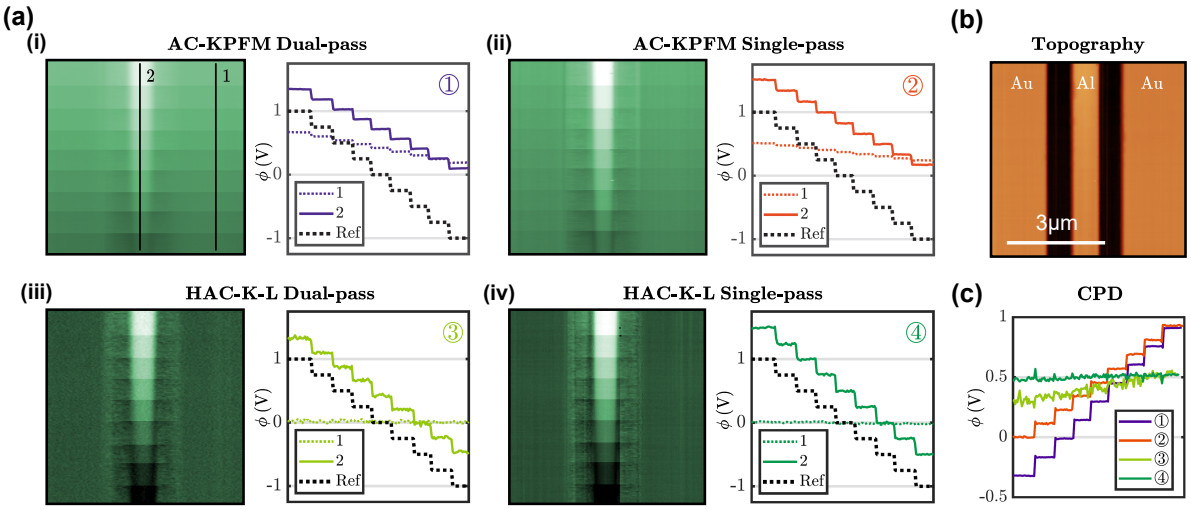

Fig. 6. (a) Sweep of the bias voltage on the aluminum pad during surface potential measurements using AC-KPFM and HAC-K-L in dual-pass and single-pass configuration (i-iv) at ambient conditions. The graphs next to the recorded images show cross-sections as indicated in (i) and the applied bias as reference. (color scale: 2 V) (b) Topography of the measured sample area with the slow scan axis disabled. (color scale: 100 nm) (c) Deviation of the measured potential difference between the two electrodes (line 1 - line 2) to the applied bias voltage. An expected constant value corresponding to the natural contact potential difference (CPD) of the metals is only observed with HAC-K-L single-pass.

Post-Print version of the article: T. Hackl, M. Poik and G. Schitter, "Heterodyne AC Kelvin Probe Force Microscopy for Nanoscale Surface Potential Imaging in Liquids," *IEEE Transaction on Instrumentation and Measurement*, 2023. DOI: 10.1109/TIM.2022.3230477

pad width: 800 nm), whose topography is shown in Fig. 6(b). Again, the Au electrode is held at ground potential, while the bias voltage on the Al-pad is swept. The cross-sections reveal the measured quantitative values of the respective measurement modes. Since only the applied potential of the Al-pad is swept, the cross-section on the Au-pad (1, dashed line) should be constant, while the cross-section of the Al-pad (2, solid line) should follow the applied bias voltage (Ref). For AC-KPFM the applied bias steps are not only observed above the Al-pad but also above the grounded Au-pad due to the poor locality of the measurement. Although, this effect reduces when measuring the surface potential simultaneously with the topography scan in (ii) (i.e. lift height = 0 nm), a clear dependence of the measured Au potential on the applied Al bias is still observable. Vice versa, the measured potential on the Al-pad does not follow accurately the applied bias (see dashed black line as reference). The resulting potential difference (Au pad - Al pad) in relation to the applied bias as shown in Fig. 6(c) is therefore not constant. Using heterodyne detection in dual-pass configuration (iii) greatly enhances the measurement accuracy but still results in a deviation from an expected constant value, which should reflect the bias-independent natural CPD of the metals. Reducing the tip-sample distance with single-pass operation (iv) not only further enhances the measurement accuracy but also increases the SNR visible in the reduced noise-level between (iii) and (iv). The extracted quantitative data is given in Table I. As discussed, a constant CPD with a minimal span and standard deviation σ is favourable. While AC-KPFM may be able to distinguish the different materials on the sample, the large influence from the applied bias voltage (CPD span of: 1232 / 926 mV) shows that it is not suitable for performing quantitative surface potential measurements at these structure sizes. Although HAC-K-L single-pass with $\bar{\sigma}$ =16.5 mV features a worse SNR than AC-KPFM ($\bar{\sigma} \cong$ 3 mV), which is caused by the heterodyne detection, its measured CPD span of 38 mV over a bias range of 2 V highlights its superior capability to quantitatively image potential distributions of nanoscale structures.

D. Surface Potential of Collagen Fibrils in Air

To further analyze HAC-K-L and to assess its applicability to biological samples, measurements on collagen fibrils are carried out and shown in Fig. 7. Collagen is the most abundant protein in mammals as it is a major component of the extracellular matrix and is therefore of great scientific interest. The topography scan (a)(i) reveals its characteristic d-banding pattern which is a result of overlapping protein fibers exhibiting gaps of well defined periodicity. Three individual fibrils of different diameter are imaged, whose height is determined to 29 nm, 55 nm and 102 nm (see cross-sections in (iii)). The simultaneously captured surface potential distribution (b) using HAC-K-L single-pass provides the same quantitative potential values irregardless of the fibrils height (iii). The fact that all fibrils show the same surface potential, despite their significant difference in height and width, indicates that the surface potential can be measured correctly. It is therefore concluded that HAC-K-L single-pass is suitable for imaging nanoscale biomolecules as it provides plausible results for structures below 100 nm width.

E. Surface Potential of Collagen Fibrils in Liquid

The main advantage of AC-KPFM over conventional KPFM is the use of a second high frequency ac voltage instead of a dc-bias for the compensation of the electrostatic force. Up to now, this dc-bias has hindered the usage of KPFM in aqueous solutions due to induced electrolysis and other parasitic electrochemical effects [28]. AC-KPFM with the extension of heterodyne detection and single-pass operation

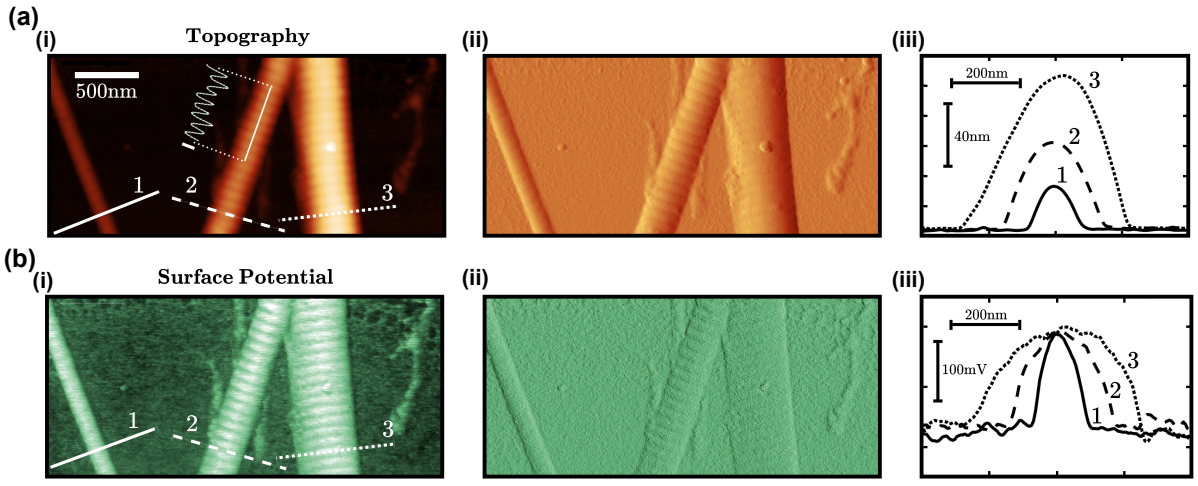

Fig. 7. (a) Topography image (i) of three individual collagen fibrils on a silicon substrate in air with the corresponding error image (ii). Cross sections (iii) of each fibril as indicated in (i). The cross section integrated in (i) visualizes the characteristic d-banding pattern of collagen (scale bar: 2 nm). (b) Surface potential (i) measured with HAC-K-L single-pass simultaneously to (a) with the corresponding error image (ii). Cross sections averaged over 5 lines (iii) of the measured potential as indicated in (i).

Post-Print version of the article: T. Hackl, M. Poik and G. Schitter, "Heterodyne AC Kelvin Probe Force Microscopy for Nanoscale Surface Potential Imaging in Liquids," *IEEE Transaction on Instrumentation and Measurement*, 2023. DOI: 10.1109/TIM.2022.3230477

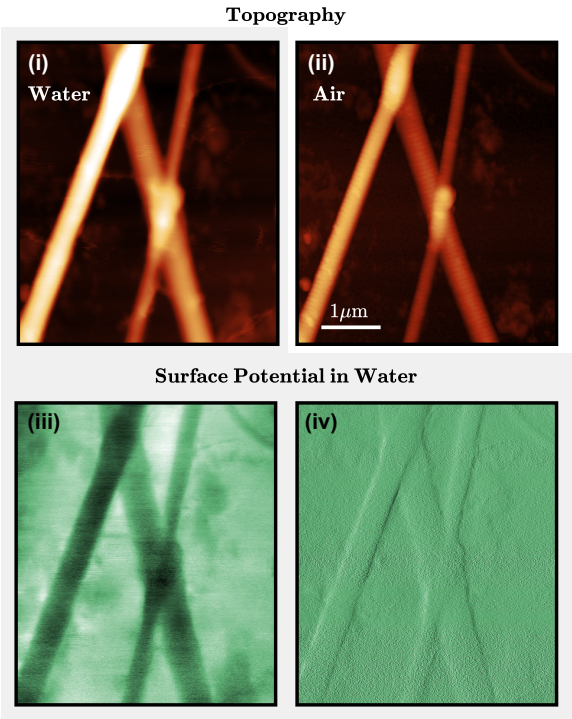

Fig. 8. Topography of several collagen fibrils measured in deionized water (i) and air (ii). (color scale: 250 nm) Simultaneously measured surface potential in deionized water using HAC-K-L (iii) with its corresponding error image (iv). (color scale: 0.3 V)

has the potential to overcome this hurdle and thus enable quantitative surface potential measurements of nanoscale structures in aqueous solutions. Figure 8 shows the measurement of the topography (i) and surface potential distribution (iii) of several collagen fibrils imaged in deionized (milli-Q) water. The topography of the same area imaged in air is given in (ii) for comparison. Due to hydration and the associated swelling of the fibrils (diameter increased by ∼48 %), the d-banding pattern is no longer observable in the topography image [29]. The measured surface potential and the corresponding error image (iv) show that stable HAC-K-L operation with nullification of the electrostatic force is possible in liquid environments. The seemingly worse noise level as compared to measurements at ambient conditions mainly originates from increased damping (lower Q factor) of the cantilever in water and the presence of mobile ions. It is expected. that this can be counteracted by increasing the measurement frequencies, in order to impede ionic motion or by using larger drive amplitudes [30].

In summary the results show, that HAC-K-L greatly increases the measurement accuracy and spatial resolution of Kelvin-probe techniques, thus enabling quantitative surface potential measurements on nanoscale biological samples such as collagen fibrils, while additionally extending its applicability to aqueous environments.

V. Conclusion

The presented heterodyne AC Kelvin-probe force microscopy mode (HAC-K-L) enables quantitative surface potential measurements of nanoscale samples in air and liquid (aqueous) environments. Due to the heterodyne detection, the mode is sensitive to electrostatic force gradients rather than forces, such as in conventional amplitude modulated KPFM modes (i.e. AM-KPFM, AC-KPFM). This makes the measurement more dependant on the localized forces at the tip apex, thus improving the spatial resolution. By additionally making use of the cantilever oscillation during the topography scan (single-pass) and therefore reduced tip-sample distances throughout the surface potential measurement, accuracy and SNR are increased further. Measurements on a gold-aluminum test sample and collagen fibrils demonstrate its capability of performing quantitative surface potential measurements of nanoscale structures, its applicability to biological samples and extension of the measurement environment to aqueous solutions. With this ability, several applications ranging from corrosion studies to glycation of collagen can be envisaged, which is part of ongoing and future work.

Acknowledgments

We thank O. Andriotis and M. Lerchbaumer from the Institute of Lightweight Design and structural Biomechanics of TU Wien for providing the collagen fibril samples.

References

[1] M. Nonnenmacher, M. P. O'Boyle, and H. K. Wickramasinghe, "Kelvin probe force microscopy," *Applied Physics Letters*, vol. 58, no. 25, pp. 2921–2923, 1991.

[2] M. Rohwerder and F. Turcu, "High-resolution kelvin probe microscopy in corrosion science: Scanning kelvin probe force microscopy (skpfm) versus classical scanning kelvin probe (skp)," *Electrochimica Acta*, vol. 53, no. 2, pp. 290–299, 2007.

[3] C. Örnek, C. Leygraf, and J. Pan, "Real-time corrosion monitoring of aluminum alloy using scanning kelvin probe force microscopy," *Journal of the Electrochemical Society*, vol. 167, no. 8, p. 081502, 2020.

[4] Y. Rosenwaks, R. Shikler, T. Glatzel, and S. Sadewasser, "Kelvin probe force microscopy of semiconductor surface defects," *Phys. Rev. B*, vol. 70, p. 085320, 2004.

[5] K. Nakazawa, K. Fukazawa, T. Uruma, G. Hashiguchi, and F. Iwata, "Imaging of an electret film fabricated on a micro-machined energy harvester by a kelvin probe force microscope," *IEEE Transactions on Instrumentation and Measurement*, vol. 71, pp. 1–7, 2022.

[6] E. Sengupta, A. L. Domanski, S. A. L. Weber, M. B. Untch, H.-J. Butt, T. Sauermann, H. J. Egelhaaf, and R. Berger, "Photoinduced degradation studies of organic solar cell materials using kelvin probe force and conductive scanning force microscopy," *The Journal of Physical Chemistry C*, vol. 115, no. 40, pp. 19 994–20 001, 2011.

[7] A. K. Sinensky and A. M. Belcher, "Label-free and high-resolution protein/dna nanoarray analysis using kelvin probe force microscopy," *Nature Nanotechnology*, vol. 2, no. 10, pp. 653–659, 2007.

[8] P. Mesquida, D. Kohl, O. G. Andriotis, P. J. Thurner, M. Duer, S. Bansode, and G. Schitter, "Evaluation of surface charge shift of collagen fibrils exposed to glutaraldehyde," *Scientific Reports*, vol. 8, no. 1, p. 10126, 2018.

[9] L. Collins, J. I. Kilpatrick, S. V. Kalinin, and B. J. Rodriguez, "Towards nanoscale electrical measurements in liquid by advanced KPFM techniques: a review," *Reports on Progress in Physics*, vol. 81, no. 8, p. 086101, 2018.

[10] G. Koley, M. G. Spencer, and H. R. Bhangale, "Cantilever effects on the measurement of electrostatic potentials by scanning kelvin probe microscopy," *Applied Physics Letters*, vol. 79, no. 4, pp. 545–547, 2001.

[11] L. Collins, S. Jesse, J. I. Kilpatrick, A. Tselev, M. B. Okatan, S. V. Kalinin, and B. J. Rodriguez, "Kelvin probe force microscopy in liquid using electrochemical force microscopy," *Beilstein Journal of Nanotechnology*, vol. 6, pp. 201–214, 2015.
[12] T. Glatzel, S. Sadewasser, and M. Lux-Steiner, "Amplitude or frequency modulation-detection in kelvin probe force microscopy," *Applied Surface Science*, vol. 210, no. 1-2, pp. 84–89, 2003.
[13] Z. M. Ma, L. Kou, Y. Naitoh, Y. J. Li, and Y. Sugawara, "The stray capacitance effect in kelvin probe force microscopy using fm, am and heterodyne am modes," *Nanotechnology*, vol. 24, no. 22, p. 225701, 2013.
[14] J. L. Garrett, M. S. Leite, and J. N. Munday, "Multiscale functional imaging of interfaces through atomic force microscopy using harmonic mixing," *ACS applied materials & Interfaces*, vol. 10, no. 34, pp. 28 850–28 859, 2018.
[15] S. Barbet, M. Popoff, H. Diesinger, D. Deresmes, D. Théron, and T. Mélin, "Cross-talk artefacts in kelvin probe force microscopy imaging: A comprehensive study," *Journal of Applied Physics*, vol. 115, no. 14, p. 144313, 2014.
[16] P. Mesquida, D. Kohl, and G. Schitter, "Signal reversal in kelvin-probe force microscopy," *Review of Scientific Instruments*, vol. 90, no. 11, p. 113703, 2019.
[17] G. Li, B. Mao, F. Lan, and L. Liu, "Practical aspects of single-pass scan kelvin probe force microscopy," *Review of Scientific Instruments*, vol. 83, no. 11, p. 113701, 2012.
[18] N. Kobayashi, H. Asakawa, and T. Fukuma, "Dual frequency open-loop electric potential microscopy for local potential measurements in electrolyte solution with high ionic strength," *Review of Scientific Instruments*, vol. 83, no. 3, p. 033709, 2012.
[19] K. Honbo, S. Ogata, T. Kitagawa, T. Okamoto, N. Kobayashi, I. Sugimoto, S. Shima, A. Fukunaga, C. Takatoh, and T. Fukuma, "Visualizing nanoscale distribution of corrosion cells by open-loop electric potential microscopy," *ACS Nano*, vol. 10, no. 2, pp. 2575–2583, 2016.
[20] Y. Zhang, X. Hu, J. Sun, Y. Shen, J. Hu, X. Xu, and Z. Shao, "High-resolution imaging and nano-manipulation of biological structures on surface," *Microscopy Research and Technique*, vol. 74, no. 7, pp. 614–626, 2011.
[21] D. Kohl, P. Mesquida, and G. Schitter, "Quantitative ac - kelvin probe force microscopy," *Microelectronic Engineering*, vol. 176, pp. 28–32, 2017.
[22] T. Hackl, G. Schitter, and P. Mesquida, "Ac kelvin probe force microscopy enables charge mapping in water," *ACS Nano*, vol. 16, no. 11, pp. 17 982–17 990, 2022.
[23] T. Hackl, M. Poik, and G. Schitter, "Dc-bias-free surface potential measurements by heterodyne ac kelvin probe force microscopy," in *2022 IEEE International Instrumentation and Measurement Technology Conference (I2MTC)*, 2022, pp. 1–5.
[24] J. L. Garrett, D. Somers, and J. N. Munday, "The effect of patch potentials in casimir force measurements determined by heterodyne kelvin probe force microscopy," *Journal of Physics: Condensed matter*, vol. 27, no. 21, p. 214012, 2015.
[25] J. L. Garrett and J. N. Munday, "Fast, high-resolution surface potential measurements in air with heterodyne kelvin probe force microscopy," *Nanotechnology*, vol. 27, no. 24, p. 245705, 2016.
[26] O. G. Andriotis, W. Manuyakorn, J. Zekonyte, O. L. Katsamenis, S. Fabri, P. H. Howarth, D. E. Davies, and P. J. Thurner, "Nanomechanical assessment of human and murine collagen fibrils via atomic force microscopy cantilever-based nanoindentation," *Journal of the Mechanical Behavior of Biomedical Materials*, vol. 39, pp. 9–26, 2014.
[27] L. Polak, S. de Man, and R. J. Wijngaarden, "Note: Switching crosstalk on and off in kelvin probe force microscopy," *Review of Scientific Instruments*, vol. 85, no. 4, p. 046111, 2014.
[28] E. AU Birkenhauer and S. AU Neethirajan, "Surface potential measurement of bacteria using kelvin probe force microscopy," *JoVE*, no. 93, p. e52327, 2014.
[29] K. Kato, G. Bar, and H. J. Cantow, "The interplay between surface micro-topography and -mechanics of type i collagen fibrils in air and aqueous media: An atomic force microscopy study," *The European Physical Journal E*, vol. 6, no. 1, pp. 7–14, 2001.
[30] T. Hackl, M. Poik, and G. Schitter, "Influence of imaging parameters on afm surface potential measurements in aqueous solutions," in *2022 IEEE 22nd International Conference on Nanotechnology (NANO)*, 2022, pp. 39–42.

Thomas Hackl received the M.Sc. degree in energy systems and automation technology from TU Wien, Vienna, Austria, in 2020, where he is currently pursuing the Ph.D. degree with the Automation and Control Institute (ACIN).
His primary research interest are on the development of advanced Atomic Force Microscopy measurement modes with the focus on KPFM and mechatronic system design.

Mathias Poik received the M.Sc. degree in energy systems and automation technology from TU Wien, Vienna, Austria, in 2017, where he is currently pursuing the Ph.D. degree with the Automation and Control Institute (ACIN).
His primary research interests are on the development of electrical Atomic Force Microscopy measurement modes, mechatronic system design, and the control of piezoelectric transducers.

Georg Schitter (Senior Member, IEEE) received the M.Sc. degree in electrical engineering from TU Graz, Graz, Austria, in 2000, and the M.Sc. and Ph.D. degrees from ETH Zürich, Zürich, Switzerland, in 2004.
He is currently a Professor for advanced mechatronic systems at the Automation and Control Institute (ACIN), TU Wien, Vienna, Austria. His primary research interests are on high-performance mechatronic systems, particularly for applications in the high-tech industry, scientific instrumentation, and mechatronic imaging systems, such as AFM, scanning laser, and LIDAR systems, telescope systems, adaptive optics, 3-D printing, and lithography systems for semiconductor industry.
Dr. Schitter received the Journal Best Paper Award of the IEEE/ASME TRANSACTIONS ON MECHATRONICS in 2017, the IFAC Mechatronics from 2008 to 2010, and the Asian Journal of Control from 2004 to 2005, and the 2013 IFAC Mechatronics Young Researcher Award. He served as an Associate Editor for IFAC Mechatronics, Control Engineering Practice, and the IEEE TRANSACTIONS ON MECHATRONICS.

Post-Print version of the article: T. Hackl, M. Poik and G. Schitter, "Heterodyne AC Kelvin Probe Force Microscopy for Nanoscale Surface Potential Imaging in Liquids," *IEEE Transaction on Instrumentation and Measurement*, 2023. DOI: 10.1109/TIM.2022.3230477